



## Article

# Evaluation of the Effects of Nano-SiO<sub>2</sub> Microemulsion on Decompression and Augmented Injection in the Eunan Tight Reservoir

Ke Wu <sup>1,2</sup>, Mingbiao Xu <sup>1,2</sup>, Shoucheng Wen <sup>1,2,\*</sup> and Xuefeng Deng <sup>3</sup>

<sup>1</sup> College of Petroleum Engineering, Yangtze University, Wuhan 430100, China; kewu0423@outlook.com (K.W.); xmb62@163.com (M.X.)

<sup>2</sup> Hubei Key Laboratory of Oil and Gas Drilling Engineering, Yangtze University, Wuhan 430100, China

<sup>3</sup> China Petrochemical North China Oil and Gas Branch Institute of Petroleum Engineering Technology, Zhengzhou 450006, China; redapple6602@126.com

\* Correspondence: 500046@yangtzeu.edu.cn

**Abstract:** The residual oil saturation of the matrix near the well zone of a tight reservoir is high due to the tight reservoir's complex conditions, such as the small pore throat radius and low permeability of the matrix and the development of microfractures, which can result in serious water channeling, even after long-term water injection development. The aim of this paper is to improve the effects of depressurization and augmented injection for tight reservoir waterflooding development by reducing the tight matrix's residual oil saturation, increasing and maintaining its water phase permeability near the well zone using a nano-SiO<sub>2</sub> microemulsion system with a small particle size and high interfacial activity. Therefore, four nano-microemulsion systems were evaluated and screened for their temperature resistance, salt resistance, interfacial tension, solubilization, and dilution resistance. A microemulsion system of 13% A + 4% B + 4% C + 4% n-butanol + 6% oil phase + 69% NaCl solution (10%) + 1% OP-5 + 0.5% anti-temperature agent + 0.3% nanosilica material was preferred. According to the core displacement experiment, the depressurization rate can reach 28~60% when the injection concentration of the system is 1~10% and the injection volume is 2~5 PV. The results of the on-site test show that the water injection pressure dropped to 17.5 MPa, which was lower than the reservoir fracture re-opening pressure. The pressure reduction rate was approximately 20%. The validity period of the depressurization and augmented injection has reached 23 months to date.



**Citation:** Wu, K.; Xu, M.; Wen, S.; Deng, X. Evaluation of the Effects of Nano-SiO<sub>2</sub> Microemulsion on Decompression and Augmented Injection in the Eunan Tight Reservoir. *AppliedChem* **2023**, *3*, 477–491. <https://doi.org/10.3390/appliedchem3040030>

Academic Editor: Raed Abu-Reiq

Received: 5 August 2023

Revised: 10 October 2023

Accepted: 14 October 2023

Published: 25 October 2023



**Copyright:** © 2023 by the authors. Licensee MDPI, Basel, Switzerland. This article is an open access article distributed under the terms and conditions of the Creative Commons Attribution (CC BY) license (<https://creativecommons.org/licenses/by/4.0/>).

## 1. Introduction

In general, the development of tight reservoirs is challenging due to low matrix permeability, complex microcracks, and high non-homogeneity [1–3]. Tight oil reservoirs have poor reservoir conditions, low matrix permeabilities, and complex fracture conditions. Despite implementing measures such as acidification and fracturing, the validity period is short. At the same time, high injection pressure can easily cause water channeling, the residual oil saturation in the near-wellbore area is still high, and the injection efficiency is poor. In this case, matrix permeability has not been improved, and the residual oil in the matrix has not been effectively expelled. These make it difficult to inject water into the matrix. The common methods of depressurization and augmented injection for tight reservoirs include acidization, water quality modification, clay shrinkage agent, etc. [4–6]. Table 1 shows the advantages and disadvantages of the common methods of depressurization and augmented injection used for tight reservoirs. Acidizing, fracturing, and other injection stimulation measures have been carried out on-site, but the stimulation effect is poor and the period of validity is short.

**Table 1.** Advantages and disadvantages of the common methods of depressurization and augmented injection for tight reservoirs.

Methods	Advantages	Disadvantages
Acidization	It can remove the blockage of the oil layer, expand and connect the pores and fractures between oil layers, and make the permeability of the oil layer near the wellbore quickly recover or increase.	Due to the heterogeneity of the reservoir, the acid is difficult to place reasonably, resulting in an increase in the formation permeability difference and the intensification of the discrepancy between the layers.
Water quality modification	Reduces the damage caused by water injected into the formation.	The construction cost is high and the period of validity is short.
Clay shrinkage agent	It avoids the damage to the formation caused by the expansion and migration of clay minerals in water, improves the effect of oil and gas development, and significantly saves on formation reconstruction costs.	The applicable formation conditions are stringent and cannot be widely used.
Nano-SiO <sub>2</sub> microemulsion	Strong adsorption capacity, high interfacial activity, strips residual oil, reduces residual oil saturation, increases water phase permeability, long action time, and can form a nanomaterial film, effectively reducing the adsorption resistance.	The high cost of a single operation.

The Chang 8 reservoir in the Honghe oil field located in the southwest of the Ordos Basin (Eunan) in China is a tight reservoir with a complex microcrack structure. The average porosity and permeability of the reservoir are 10% and  $0.4 \times 10^{-3} \mu\text{m}^2$ , respectively. The average pore radius is only 0.21  $\mu\text{m}$ , and the connectivity between the pores is poor. These characteristics make it difficult to inject water into the matrix [7–10]. On the other hand, the microcrack re-opening pressure of the Chang 8 reservoir is approximately 18–25 MPa according to laboratory experiments. With the implementation of waterflood development, the injection pressure rose rapidly to 22.9 MPa within 6 months, which approached or exceeded the microcrack re-opening pressure. As a result, water channeling is serious, and the residual oil saturation in the matrix near the water injection well is still at a high level. This greatly reduces the effectiveness of waterflood development. According to Figure 1, the relative permeability curve of the Chang 8 reservoir, the Krw increases from 40.347% to 68.07% if residual oil saturation decreases by 10%. This increase in the percentage of Krw is more than 60%. It is necessary to decrease the residual oil saturation and increase the aqueous permeability of the matrix near the bore because the seepage resistance is mainly concentrated in this area. Therefore, a nano-SiO<sub>2</sub> microemulsion was adopted because of its small particle size (1–100 nm) and high interfacial activity [11,12]. This work aims to screen the nano-SiO<sub>2</sub> microemulsion system for the Eunan tight reservoir by evaluating its anti-temperature, anti-salt, solubilization, and dilution resistance properties, which affect the sweeping oil efficiency and processing radius of the system. Laboratory and on-site tests proved that the system effectively reduces pressure and increases injection in the tight reservoir in Eunan.

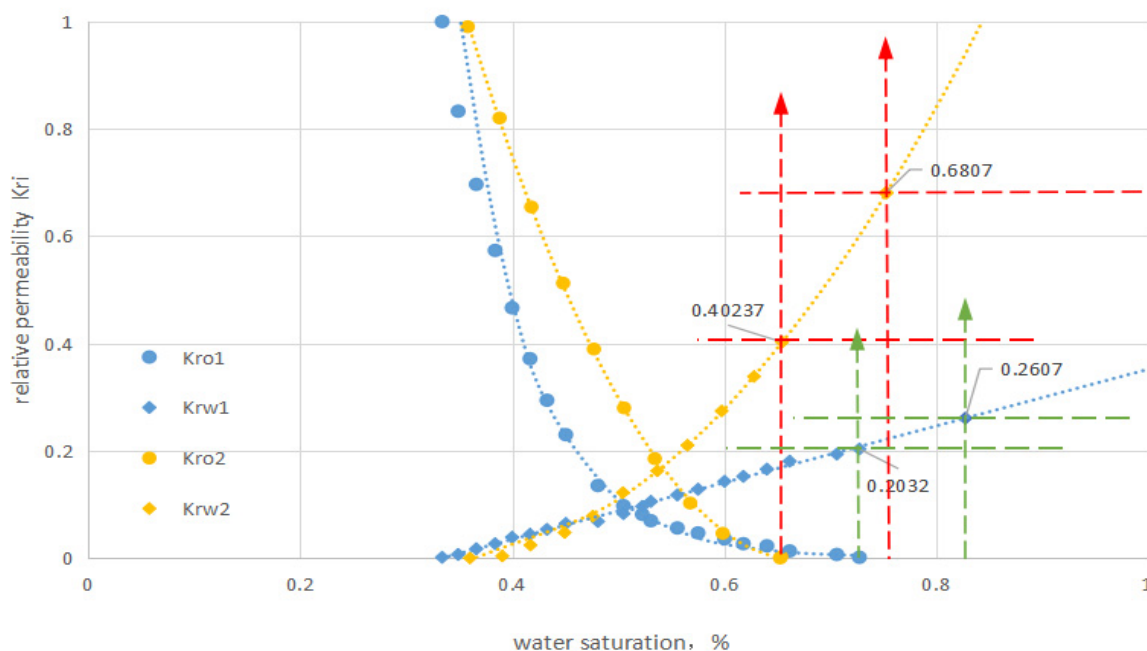


**Figure 1.** Chang 8 reservoir oil–water relative permeability curve.

## 2. Nano-SiO<sub>2</sub> Microemulsion Decompression and Augmented Injection Mechanism

The nano-SiO<sub>2</sub> microemulsion decompression and augmented injection mechanisms are mainly developed from the following perspectives:

- (a) Reduce oil–water interfacial tension, increase the flow capacity of crude oil

A large amount of residual oil is distributed in the rock sample, and the microemulsion can reduce the oil–water interfacial tension and increase the wetting angle of oil on the rock surface, so it will make the bond strength and surface energy of oil droplets decrease, which is beneficial to the subsequent oil-washing ability [13]. The adsorption effect of surfactants on the oil–water interface leads to the reduction of oil–water interfacial tension, the adhesion work required to strip the crude oil is reduced, the residual oil droplets easily flow, the flow capacity of crude oil becomes stronger, and the efficiency of oil repulsion is improved, so as to achieve the purpose of reducing the pressure and increasing the injection [14].

- (b) Increase the number of capillary tubes to improve the efficiency of oil repelling

The capillary quotient, also known as the capillary count or critical repulsion ratio, represents the ratio of the capillary force on the viscous force to the repulsive force. Reduced oil–water interfacial tension can increase the capillary quotient, thus reducing the capillary resistance of the formation, resulting in the decrease in residual oil saturation and the increase in oil drive efficiency [15].

$$N_c = \frac{\mu_w V_w}{\varphi \sigma_{ow}}$$

In the formula:  $N_c$ —capillary quotient;

$\mu_w$ —repellent fluid viscosity, mPa·s;

$V_w$ —repulsion rate, m/s;

$\sigma_{ow}$ —interfacial tension between oil and repellent fluid, mN/m.

- (c) Enhance the solubilizing and dispersing effect

Crude oil on the surface is rapidly dispersed and separated under shear, forming an oil/water emulsion. As the mobility increases, the wave coefficient also increases significantly. In addition, the adsorption effect of the nano-SiO<sub>2</sub> microemulsion makes it

difficult for oil droplets with the same charge to coagulate and are eventually entrained and driven out by the active water, thus improving the oil-washing efficiency [16].

#### (d) Reverse wettability

Nanoparticle suction can be adsorbed on the rock surface, reducing the solid–liquid interfacial energy and increasing the contact angle of the crude oil on the surface, further enhancing the degree of rock wetting and thus reducing its binding effect on crude oil, stripping residual oil, and reducing residual oil saturation. Microscopically, it enhances the oil-driving efficiency and the effect of lowering pressure and increasing injection.

Nanomaterials have strong adsorption ability and high interfacial activity, which can enter the micro- or even nanopores, strip residual oil, and reduce the residual oil saturation and long action time [17], but they easily spontaneously gather in the solution, which seriously affects the construction effect [18,19]. Surfactant interfacial activity is high, but its adsorption capacity is relatively weak [20,21], and the emulsion particles gradually increase with the increase in the amount of emulsified oil, which can lead to Jamin's effect, affecting the effect of decompression and augmented injection [22]. In addition, the microemulsion itself has ultra-low interfacial tension and rock wettability transformation [23–25], reducing the binding energy of the rock to the crude oil, and thus the oil-washing efficiency is improved [26,27]. It also has a strong dispersion performance for nanomaterials. The nano-SiO<sub>2</sub> microemulsion can reduce the residual oil saturation and increase the water phase permeability. After reducing the residual oil saturation, the amphiphilic nanomaterials can be tightly adsorbed on the inner surface of the rock to form a nanomaterial membrane, which effectively reduces the adsorption resistance and effective time will be long, which reduces the operation cost to a certain extent. Therefore, for tight reservoirs, nanomaterials are usually compounded with surfactants, and the synergistic effect of nanoparticles and microemulsions can be used to further enhance the effect of decompression and augmented injection.

### 3. Materials

#### *Experimental Apparatus and Reagents*

An MS12001L/02 electronic balance, J-HH-4A electric thermostatic water bath, ultralow interfacial tension meter, and HKY-1 multifunctional core expulsion device were used.

The drugs involved in this experiment include AP6, polyoxyethylene surfactant, petroleum sulfonate, n-butanol, oil phase, NaCl solution, anti-temperature drugs, and nanosilica materials. Except for the nano-SiO<sub>2</sub> microemulsion, all drugs involved in the experiments were analytically pure. Table 2 shows the water properties of the Chang 8 reservoir formation in the HH12 well area.

**Table 2.** Data table for formation water analysis in the HH12 well area, Chang 8 reservoir.

Stratum	Cl <sup>−</sup> (mg/L)	Mineralization (mg/L)	Water Type
Chang 8	37,874	61,246	CaCl <sub>2</sub>

The rock particles of the Chang 8 reservoir in Honghe Oilfield are mainly fine-grained and medium-fine-grained clastic feldspar sandstone. The cementation type is mainly pore type and occasionally film type. Particle support is mainly based on particle support, supplemented by particle mixed base support; the contact mode is mainly point-line-surface contact.

The reservoir core of the HH12 well area was selected for composition analysis. The lithology of reservoir sandstone is mainly fine sand and medium sand, and the rock types of reservoir sandstone are mainly gray and dark gray feldspar clastic sandstone and rock clastic feldspar sandstone.

The detrital components of sandstone are mainly quartz and feldspar, the average content of quartz is 32.08%, the average content of feldspar is 29.01%, followed by rock debris, the average content of which is 23.39%, mainly igneous rock, and metamorphic rock

debris. The content of clay minerals is 11.76%, which contains mainly chlorite (accounting for 39.79%) and kaolinite (accounting for 27.85%), and a certain proportion of mica, with an average content of 3.76% (refer to Figure 2).

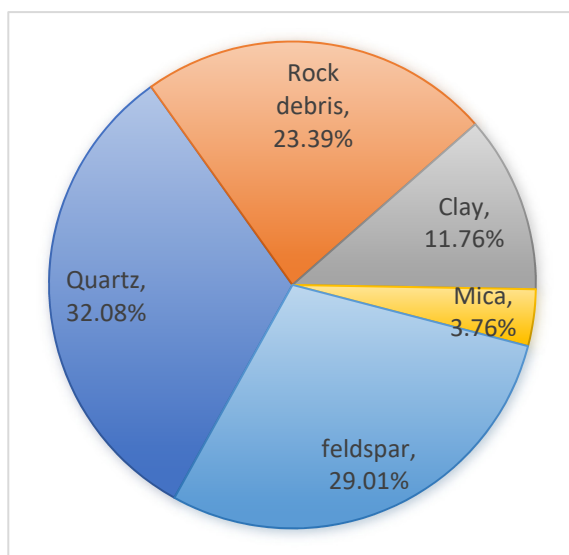


**Figure 2.** Lithologic composition of reservoir core.

According to the results of laboratory experiments, the acid in the Chang 8 reservoir in the HH12 well area caused no damage to the permeability and instead has improved it. The reservoir sensitivity as a whole represents weak acid sensitivity, weak stress sensitivity, weak water sensitivity, weak alkali sensitivity, and moderately weak quick sensitivity. The rock brittleness index of the Chang 8 reservoir in the HH12 well area is 50.7%.

#### 4. Experiments

##### 4.1. Nano-SiO<sub>2</sub> Microemulsion System Preference and Performance Evaluation

###### 4.1.1. Temperature Resistance Test

The four nano-SiO<sub>2</sub> microemulsions, c8-A, c8-B, c8-C, and c8-D, were diluted with formation water at the ratios of 1:1, 1:2, 1:4, 1:9, and 1:19, respectively, and placed at reservoir temperature (70 °C) for 24 h to examine their stability.

###### 4.1.2. Anti-Dilution Performance Test

The four nano-SiO<sub>2</sub> microemulsion systems, c8-A, c8-B, c8-C, and c8-D, were diluted with tap water in the ratios of 1:1, 1:2, 1:4, 1:9, and 1:19 respectively, and left at 70 °C for 24 h.

###### 4.1.3. Salt Resistance Test

The four nano-SiO<sub>2</sub> microemulsion systems with a mass fraction of 10% were mixed with groundwater in different proportions by taking 20 mL and placed at 70 °C for 24 h to observe the experimental phenomena.

###### 4.1.4. Interfacial Tension Test

The interfacial tension between c8-C and c8-D was measured by diluting them to 10% with formation water.

###### 4.1.5. Solubilization Performance Test

First, 30 mL of 10% or 20% nano-SiO<sub>2</sub> microemulsion was added to a stoppered graduated cylinder, and then 30 mL of Chang 8 reservoir crude oil was added. Then, the samples were sealed and shaken and kept at a constant temperature of 70 °C in a water bath for 24 h.

#### 4.1.6. Oil-Washing Performance Test

First, 50 g of 20–40 mesh quartz sand was mixed with 2 g of Chang 8 reservoir crude oil and sealed in a drying oven at 70 °C for 48 h. Then, 1%, 5%, and 10% c8-C solutions were configured with stratigraphic water, tap water, and 1% potassium chloride solution, respectively. Three 25 mL colorimetric tubes were filled with 2 g of oil sand and 20 mL of the above-mentioned different concentrations of nano-SiO<sub>2</sub> microemulsion solution, sealed with a plug, and put into a 70 °C water bath at a static constant temperature for 24 h. After 24 h, they were removed and cold water was used to remove the residual nano-SiO<sub>2</sub> microemulsion and other working solutions from the surface of the oil sand, then the cleaned oil sand was dried and weighed.

#### 4.2. Evaluation Experiments on the Effect of Indoor Core Drive Decompression

Experimental methods: (1) Saturated core with simulated formation water for vacuum pumping; (2) the core is saturated with crude oil and displaced to the residual oil state; (3) microemulsion slug is injected and placed for 12 h; (4) finally, the trend of injection pressure change is obtained by displacement of formation water.

The working fluid of nano-SiO<sub>2</sub> microemulsion was diluted and configured with formation water to explore the effect of nano-SiO<sub>2</sub> microemulsion concentration and injection volume on the effect of decompression. The following Table 3 shows the natural core parameters.

**Table 3.** Core data.

Number	Length L/cm	Diameter D/cm	Gas Permeability Kg/md
10	8.198	2.500	0.46
14	8.086	2.504	61.59

Note: The physical properties, mineralogical characteristics, and clay content of natural cores affect the adsorption properties of nanomaterials and surfactants, and the establishment of residual oil saturation also affects the injection pressure. Therefore, there are uncertainties as well as some errors in this experiment.

## 5. Results

### 5.1. Nano-SiO<sub>2</sub> Microemulsion Performance Tests

#### 5.1.1. Temperature Resistance Test

The experimental results showed that the four nano-SiO<sub>2</sub> microemulsion systems maintained a clarified state after 70 °C and 24 h without micelle destruction, indicating that the above systems have good temperature resistance.

#### 5.1.2. Anti-Dilution Performance Test

The results showed that all four nano-SiO<sub>2</sub> microemulsion systems did not weaken the microemulsion system, indicating that all four nano-SiO<sub>2</sub> microemulsion systems have good anti-dilution properties, which is beneficial to maximize the treatment radius. Table 4 shows the results of the anti-dilution performance of nano-SiO<sub>2</sub> microemulsion c8-A~c8-D.

#### 5.1.3. Salt Resistance Test

The results are shown in the following Table 5.

Compared with the experiments using clear water dilution, the high salt concentration has a certain degree of influence on the anti-dilution stability of the nano-SiO<sub>2</sub> microemulsion systems. As can be seen from Table 4, the four nano-SiO<sub>2</sub> microemulsion systems have good compatibility with the formation water and strong salt resistance. Among them, c8-C maintains good stability after diluting nearly 20 times with highly saline formation water in the Chang 8 reservoir in the Honghe Oilfield, which can meet the requirement of the application environment of this oilfield and is more conducive to maximizing the treatment radius.

**Table 4.** Nano-SiO<sub>2</sub> microemulsion c8-A~c8-D anti-dilution performance test results statistics table.

Dilution Ratio	1:1	1:2	1:4	1:9	1:19
c8-A					
c8-B					
c8-C					
c8-D					

#### 5.1.4. Interfacial Tension Test

The interfacial tension results are shown in Table 6.

The experimental results show that c8-C and c8-D have certain interfacial reduction functions, in which the interfacial tension of a 10% c8-C nano-SiO<sub>2</sub> microemulsion system can be reduced to 10<sup>-2</sup> mN/m.

#### 5.1.5. Solubilization Performance Test

The results of the solubilization test are shown in Tables 7 and 8.

The crude oil enters the micelles in the form of tiny droplets, thus achieving the purpose of solubilization. The results show that the nano-SiO<sub>2</sub> microemulsion system c8-C has good solubilization performance for Chang 8 oil samples, with an average solubilization amount of 6.5 mL/30 mL.

Combining the above evaluations, the c8-C nano-SiO<sub>2</sub> microemulsion system was finally selected with the following composition: 13% A + 4% B + 4% C + 4% n-butanol + 6%

oil phase + 67.2% NaCl solution (10%) + 1% OP-5 + 0.5% anti-temperature agent + 0.3% nanosilica material.

**Table 5.** Nano-SiO<sub>2</sub> microemulsion salt resistance test.

Nano-SiO <sub>2</sub> Microelectronics	10% Nano-SiO <sub>2</sub> Microemulsion Volume/mL	Stratigraphic Water Volume/mL	Status
c8-A	20 mL	1 mL	Homogeneous solution, no turbidity, no precipitation
		5 mL	Homogeneous solution, no turbidity, no precipitation
		10 mL	Homogeneous solution, no turbidity, no precipitation
		15 mL	There is white oil precipitation, and oil film appears on the surface of the solution
c8-B	20 mL	1 mL	Homogeneous solution, no turbidity, no precipitation
		5 mL	Homogeneous solution, no turbidity, no precipitation
		10 mL	Homogeneous solution, no turbidity, no precipitation
		15 mL	There is white oily precipitation
c8-C	20 mL	1 mL	Homogeneous solution, no turbidity, no precipitation
		5 mL	Homogeneous solution, no turbidity, no precipitation
		10 mL	Homogeneous solution, no turbidity, no precipitation
		15 mL	Homogeneous solution, no turbidity, no precipitation
		20 mL	Homogeneous solution, no turbidity, no precipitation
c8-D	20 mL	1 mL	Homogeneous solution, no turbidity, no precipitation
		5 mL	Homogeneous solution, no turbidity, no precipitation
		10 mL	Homogeneous solution, no turbidity, no precipitation
		15 mL	Homogeneous solution, no turbidity, no precipitation
		20 mL	There is an earthy yellow oily precipitation

**Table 6.** Results of 10% nano-SiO<sub>2</sub> microemulsion interfacial tension.

Project	Number of Tests	Interfacial Tension/(mN/m)	Average/(mN/m)
c8-C	1	0.0489	0.03733
	2	0.0406	
	3	0.0325	
	4	0.0273	
c8-D	1	0.14	0.144
	2	0.133	
	3	0.165	
	4	0.138	

**Table 7.** Nano-SiO<sub>2</sub> microemulsion solubilization performance test results.

Nano-SiO <sub>2</sub> Microemulsion Type	Number of Tests	Volume before Solubilization/mL		Volume after Solubilization/mL		Solubilized Oil Phase Volume/mL
		Nano-SiO <sub>2</sub> Microemulsion /mL	Oil Phase/mL	Nano-SiO <sub>2</sub> Microemul- sion/mL	Oil Phase/mL	
c8-C (10%)	1	30	30	35	25	5
	2	30	30	38	22	8
c8-C (20%)	1	30	30	37	23	7
	2	30	30	35	25	5
c8-D (10%)	1	30	30	31	29	1
	2	30	30	34	26	4
c8-D (20%)	1	30	30	32	28	2
	2	30	30	32.5	27.5	2.5

**Table 8.** Nano-SiO<sub>2</sub> microemulsion solubilization performance test result pattern.

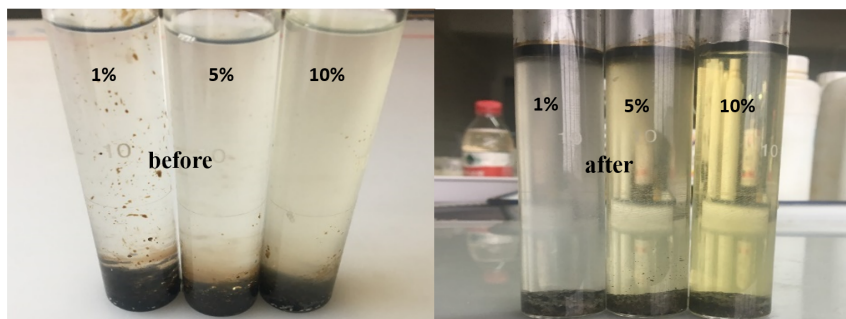
Project	10% Nano-SiO <sub>2</sub> Microemulsion Volume	20% Nano-SiO <sub>2</sub> Microemulsion Volume
c8-C		
c8-D		

#### 5.1.6. Oil-Washing Performance Test

The results of the experiment are shown in Table 9 below. Figures 3–5 show the effect of different oil-washing working fluids on oil washing.

**Table 9.** Effect of oil washing with different solution dilutions of nano-SiO<sub>2</sub> microemulsion.

Solution Type	Nano-SiO <sub>2</sub> Microemulsion Concentration/%	Oil Sand Quality (before Experiment)/g	Oil Sand Quality (after Experiment)/g	Washing Oil Efficiency
Stratigraphic water	1%	2	1.77	12%
	5%	2	1.75	13%
	10%	2	1.71	15%
Tap water	1%	2	1.84	8%
	5%	2	1.83	9%
	10%	2	1.81	10%
1% KCL	1%	2	1.84	8%
	5%	2	1.82	9%
	10%	2	1.79	11%

**Figure 3.** Experiment of oil-washing effect on diluted nano-SiO<sub>2</sub> microemulsion of stratigraphic water.

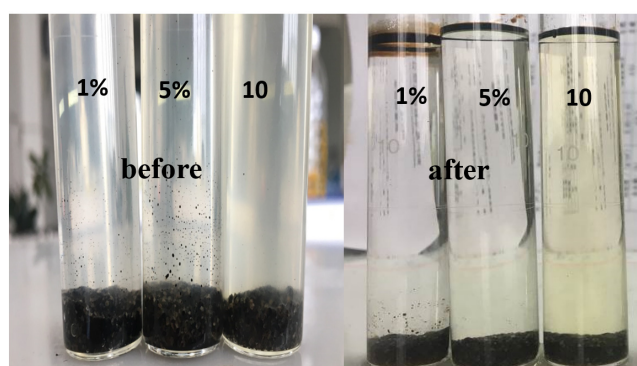


**Figure 4.** Experiment of oil-washing effect of tap water dilution on nano-SiO<sub>2</sub> microemulsion.

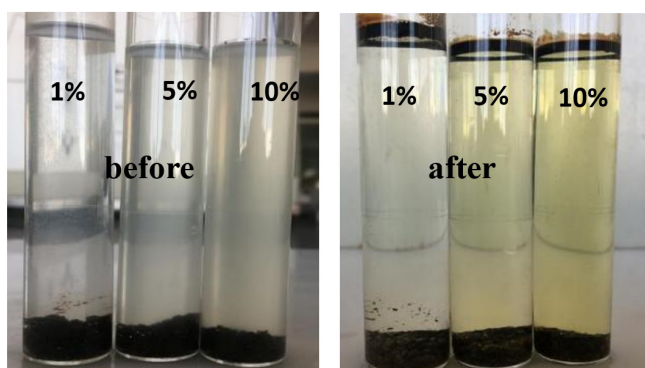


**Figure 5.** Experiment of oil-washing effect of 1% potassium chloride dilution on nano-SiO<sub>2</sub> microemulsion.

The experimental results show that the nano-SiO<sub>2</sub> microemulsions configured with tap water, stratum water, and 1% potassium chloride solution, respectively, have certain oil-washing abilities, and the nano-SiO<sub>2</sub> microemulsion configured with stratum water has the best oil-washing effect.

### 5.2. Core Displacement Depressurization Effect Evaluation Experiment

Table 10 and Figures 6 and 7 show the experimental results for 1% and 10% nano-SiO<sub>2</sub> microemulsions with an injection volume of 5 PV. Table 11 shows the experimental results for 1% and 10% nano-SiO<sub>2</sub> microemulsions with injection volumes of 2 PV and 5 PV, respectively.

**Table 10.** Hypotensive effect of different concentrations of nano-SiO<sub>2</sub> microemulsion.

Nano-SiO <sub>2</sub> Microemulsion Concentration/%	Core Permeability/ $10^{-3} \mu\text{m}^2$	Residual Oil Repulsion Pressure/MPa	Improving Post-Replacement Stress/MPa	Decompression Rate/%
10%	0.33	1.65	0.65	60.6%
1%	0.47	0.715	0.39	45.5%

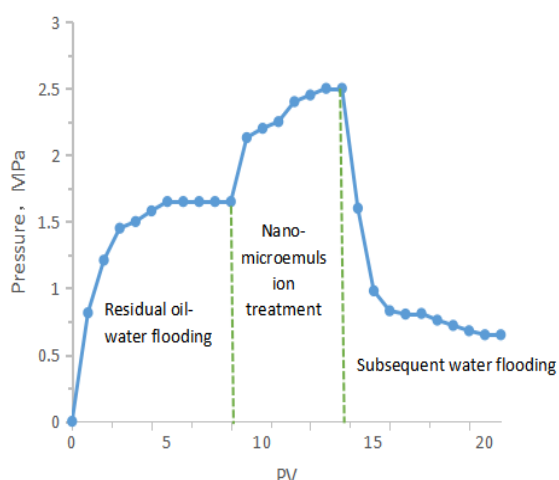


**Figure 6.** Differential pressure curve of 5 PV repulsion for 10% nano-SiO<sub>2</sub> microemulsion injection.

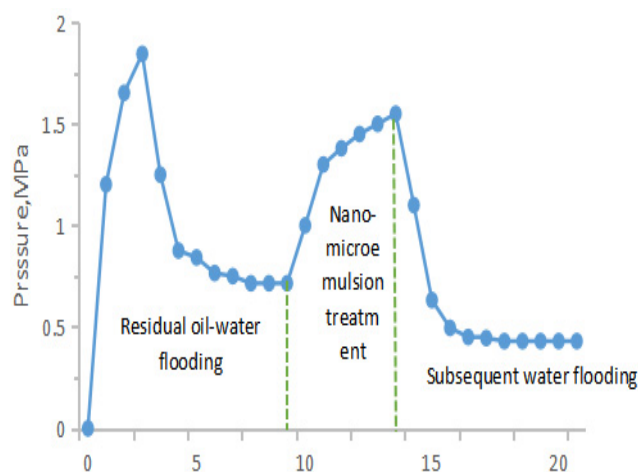


**Figure 7.** Differential pressure curve of 5 PV repulsion with 1% nano-SiO<sub>2</sub> microemulsion injection.

**Table 11.** Hypotensive effect of nano-SiO<sub>2</sub> microemulsion with different injection volumes.

Nano-SiO <sub>2</sub> Microemulsion Concentration/%	Core Permeability/ $(10^{-3} \mu\text{m}^2)$	Injected Volume/PV	Residual Oil Repulsion Pressure/MPa	Improving Post-Replacement Stress/MPa	Decompression Rate/%
1%	0.41	2	2.02	1.45	28.2%
1%	0.47	5	0.715	0.39	45.5%
10%	0.49	2	2.84	1.56	45.1%
10%	0.33	5	1.65	0.65	60.6%

From the above experimental results, it can be seen that the buckling rate of nano-SiO<sub>2</sub> microemulsion is related to the nanoemulsion injection concentration and injection volume. The decompression rate was 28.2% and 45.5% with the injection of 2 PV and 5 PV volumes and 1% nano-SiO<sub>2</sub> microemulsion injection concentration, respectively. The decompression rates are 45.1% and 60.6% for nano-SiO<sub>2</sub> microemulsion injected at 10% and 2 PV and 5 PV volumes, respectively. It can be seen that c8-C is effective in lowering pressure and increasing injection.

## 6. Field Test and Effect Analysis of Depressurization and Augmented Injection

### 6.1. Well History and Injection Well Production

Well X was fractured and put into production in September 2012. The initial daily fluid production was 33.7 t, and the water cut was 100%. Before the water injection, the daily

fluid production was 2.8 t, the daily oil production was 0.1 t, and the water cut was 95%. In May 2014, from pumping to injection, the initial daily injection volume was  $45 \text{ m}^3/\text{d}$ , and the oil pressure rose rapidly to 21.5 MPa. To reduce the injection pressure, the daily water injection volume was reduced to about  $20 \text{ m}^3$ , but the injection pressure was still maintained above 20 MPa. In July 2016, the injection was stopped, and production was restarted in May 2018. The daily injection volume was  $20 \text{ m}^3/\text{d}$ , the initial oil pressure was 10 MPa, and the water injection pressure rose rapidly to 22.6 MPa with the extension of the production time, which was close to the maximum pressure-bearing capacity of the equipment (23 MPa), and the bottom hole pressure was close to or exceeded the formation fracture pressure (30.5~35.4 MPa). The Chang 8 reservoir is a weak hydrophilic reservoir with low matrix permeability and high residual oil saturation (27.4%), which seriously affects the reservoir matrix water absorption capacity. Therefore, we consider injecting nanomicroemulsion to reduce the residual oil saturation of the matrix in the near-well zone, unblock its percolation and filtration channel, improve the reservoir matrix water absorption capacity, reduce the injection pressure, and prevent fracture water runaway to improve the water injection development effect.

## 6.2. Construction Parameter Design

According to the indoor experiment, the formation of a water-diluted nano-SiO<sub>2</sub> microemulsion was used as the working fluid in the field test, and the dilution concentration is 10%. Because of its low interfacial tension and excellent solubilization and oil-washing performance, it can minimize the residual oil saturation in the reservoir matrix near the wellbore zone. At the same time, due to its strong anti-dilution ability, it is beneficial to maximize the processing radius. On the other hand, to reduce the operation cost, the processing radius of 2 m and the injection volume of 1 PV are designed. To compare the displacement effect of nano-SiO<sub>2</sub> microemulsion and water flooding, the initial daily injection amount of nano-SiO<sub>2</sub> microemulsions was designed to be consistent with the daily injection amount of fresh water before the shut-in of Well X, according to  $20 \text{ m}^3/\text{d}$ .

The dosage of the segment plug is calculated according to the following formula:

$$V = \pi(R_2^2 - R_1^2) \cdot h \cdot \phi \cdot \beta$$

in the formula:

$V$ —the amount required for each segment plug,  $\text{m}^3$ .

$R_2$ —external ring radius of different segment plugs, m,  $R_2 = 2.05$ .

$R_1$ —inner ring radius of different section plugs, m,  $R_1 = 0.05$  ( $4\frac{1}{2}$  casing inner diameter 0.1 m).

$h$ —thickness of the reservoir, m.

$\phi$ —porosity.

$\beta$ —pore volume multiplier, here is 1.

The dosage is calculated by using the volume of the horizontal section as the axis for a horizontal section of the cylinder; the horizontal section is 584 m and the treatment radius is 2 m. The dosage of the nano-SiO<sub>2</sub> microemulsion agent is calculated as shown in Table 12 below.

**Table 12.** Well X nano-SiO<sub>2</sub> microemulsion decompression and augmented injection dosage design.

Treatment	Horizontal Section Length/m	Porosity	$\beta/\text{PV}$	$R_2/\text{m}$	$R_1/\text{m}$	Dosage/ $\text{m}^3$
c8-C nano-SiO <sub>2</sub> microemulsion	548	0.053	1	2.05	0.05	383

## 6.3. Field Application

The following Figure 8 shows the production data for Well X from March 2018 to February 2023.

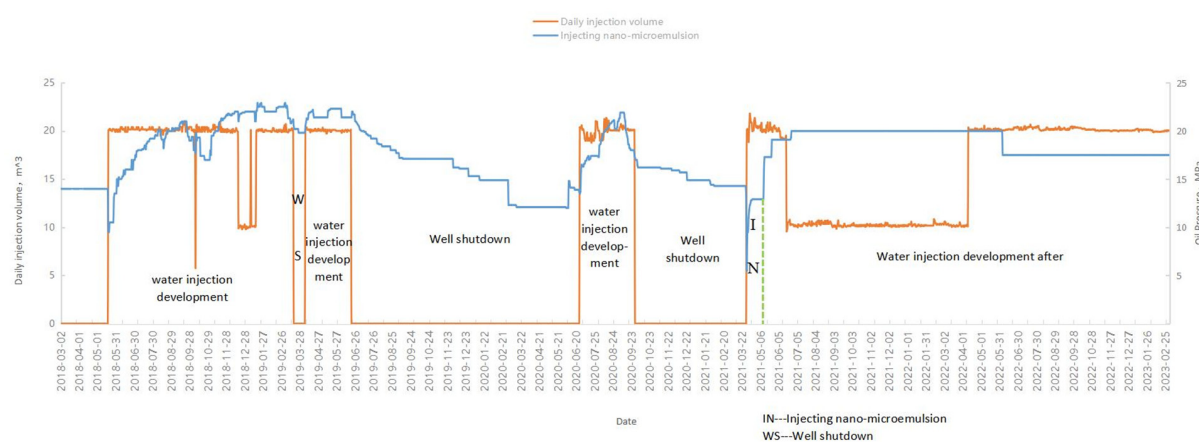


**Figure 8.** Production data of Well X group.

The well was dispensed at  $20\text{ m}^3$  in May 2018 with an oil pressure of 9.50 MPa. The oil pressure increased significantly during the injection process. After only 6 months, the oil pressure rose to 22.90 MPa, exceeding the fracture re-opening pressure and close to the formation rupture pressure. In November 2018, the daily injection volume was reduced to  $10\text{ m}^3$  in order to reduce the injected oil pressure, but the oil pressure remained above 20 MPa, forcing the well to be shut in and shut down in March 2019. After that, water injection was put into production twice, between April 2019 and June 2019 and in June 2020. In September 2020, with a daily allotment of  $20\text{ m}^3$  and a sharp increase in injection pressure, both were forced to stop due to excessive injection pressure (up to 21.9 MPa). On 21 April 2021, the operation of nano-SiO<sub>2</sub> microemulsion decompression and augmented injection measures was implemented, with  $20\text{ m}^3$  of 10% nano-SiO<sub>2</sub> microemulsion dispensed daily and a total of  $380\text{ m}^3$  dispensed, and the injection pressure was always maintained at 12.90 MPa. After the operation, the maximum water injection oil pressure is 20.0 MPa; up to now, the daily dispensing volume is  $20\text{ m}^3$ , and the water injection oil pressure is reduced to 17.5 MPa; the decompression rate reaches about 20% and it has been running continuously and smoothly for nearly 23 months.

The nano-SiO<sub>2</sub> microemulsion system is effective in decompression and augmented injection, which can effectively improve the recovery rate; at the same time, it significantly reduces the operating cost of the oilfield and increases the profit of the field. The following Table 13 shows the comparison of operation costs between ordinary microemulsions and nano-SiO<sub>2</sub> microemulsions. It shows that although the operation cost of the nano-SiO<sub>2</sub> microemulsion is higher, it is more effective and has a longer validity period and it needs to be used only once in every two years.

**Table 13.** The construction cost comparison between normal microemulsion and nano-SiO<sub>2</sub> microemulsion.

Drug dosage/PV Unit: t	Drug price w/t	Program: 10% × 2 PV	Single cost price/w	Single validity period/m	Number of operations in 2 years	Total cost of operations /w
Common microemulsion	108.57	3.2	694.85	6 [28]	4	2779.39
Nano-SiO <sub>2</sub> microemulsion	103.23	3.65	753.57	23	1	753.57

Overall, the nano-SiO<sub>2</sub> microemulsion system is effective in decompression and augmented injection in tight reservoirs, and it greatly reduces the operation cost and increases the field profit.

## 7. Conclusions

This article studies the high-pressure injection of tight oil reservoirs in southern Hubei. The nano-SiO<sub>2</sub> microemulsion system was prepared by the Schulman method in the laboratory, and its temperature resistance, salt resistance, interfacial tension, solubilization, dilution resistance, and other properties were evaluated and screened. At the same time, indoor and field experiments were carried out, and the following conclusions were drawn:

1. The preferred nano-SiO<sub>2</sub> microemulsion formula is: 13% A + 4% B + 4% C + 4% n-butanol + 6% oil phase + 67.2% salt solution + 1% OP-5 + 0.5% anti-temperature agent + 0.3% nano-SiO<sub>2</sub> material. The SiO<sub>2</sub> microemulsion system can withstand high temperatures of 70 °C, with excellent anti-temperature performance; it can withstand more than 20 times volume dilution, with good anti-dilution performance. The system has excellent anti-salt performance and stable and non-emulsion breakage in the environment of high mineralization of formation water, which is conducive to the maximization of the treatment radius. The lowest interfacial tension can reach 0.0273 mN/m; the average solubilization volume can reach 6.5 mL/30 mL; and the oil-washing efficiency can reach 15%.
2. The core replacement experiments illustrate that nano-SiO<sub>2</sub> microemulsions are effective in reducing the injection pressure in low-permeability cores. The c8-C nano-SiO<sub>2</sub> microemulsion system has a lower dilution ratio and a larger injection volume, and the decompression efficiency is better. The injection of a 2 PV mass fraction of 10% nano-SiO<sub>2</sub> microemulsion can reduce the injection pressure by 45.1%.
3. The field test results show that after the injection of the nano-SiO<sub>2</sub> microemulsion system, the daily injection volume is 20 m<sup>3</sup> and the maximum water injection oil pressure is 20.0 MPa. Up to now, the oil pressure of water injection has been reduced to 17.5 MPa, and the decompression rate is about 20%. It has been running smoothly for nearly 23 months, indicating that the system has an obvious effect on reducing pressure and increasing injection in low-permeability tight reservoirs and can effectively improve the oil recovery rate.

**Author Contributions:** Validation, S.W.; formal analysis, X.D.; investigation, K.W.; resources, M.X.; data curation, K.W.; writing—original draft preparation, K.W.; writing—review and editing, S.W.; supervision, M.X.; project administration, X.D. All authors have read and agreed to the published version of the manuscript.

**Funding:** This research was supported by the Open Fund of Hubei Provincial Key Laboratory of Oil and Gas Drilling (YQZC202105) and Production Engineering and the Project Fund of Hubei Provincial Key R&D Program (2020BAB072).

**Institutional Review Board Statement:** Not application.

**Informed Consent Statement:** Not application.

**Data Availability Statement:** Data are available upon request due to limitations such as privacy or ethics. The data provided in this study are available from the corresponding author upon request. The data are not publicly available due to on-site production.

**Conflicts of Interest:** Author Xuefeng Deng was employed by the company China Petrochemical North China Oil and Gas Branch Institute of Petroleum Engineering Technology. The remaining authors declare that the research was conducted in the absence of any commercial or financial relationships that could be construed as a potential conflict of interest.

## References

1. Wang, B.P.; Cao, M.L.; Li, D.L.; Chen, Y.B. Predictive Study of Interrift Pressure Field Interference for Density Oil Production Capacity. *Unconv. Oil Gas* **2019**, *6*, 60–64.
2. Li, G.X.; Lei, Z.D.; Dong, W.H.; Wang, H.Y.; Zheng, X.F.; Tan, J. Progress, challenges and prospects of unconventional oil and gas development in China. *China Pet. Explor.* **2022**, *27*, 1–11.
3. Kang, Y.L.; Tian, J.; Luo, P.Y.; You, L.J.; Liu, X.F. Technical bottlenecks and development strategies for enhanced recovery in tight oil reservoirs. *J. Pet.* **2020**, *41*, 467–477.

4. Wei, F.; Acosta, E.; Gawas, K.; Pushkala, K. Targeting High Molecular Weight Wax. In Proceedings of the SPE International Symposium on Oilfield Chemistry, The Woodlands, TX, USA, 13–15 April 2015.
5. Zhao, Y.J.; Hou, J.R.; Qu, M.; Xiao, L.X.; Liu, Y.B. Performance evaluation and oil drive mechanism analysis of nano-microemulsions in tight reservoirs. *Oilfield Chem.* **2022**, *39*, 338–342+354.
6. Zhou, D.; Xiong, X.D.; He, J.B.; Dong, B.; He, Y. Multi-stage steering fracturing technology for low permeability reservoirs. *Pet. Drill. Technol.* **2020**, *48*, 85–89.
7. Yang, S.; Li, C.X.; Liu, D.W.; Deng, Z.A.; Yang, F.; Sun, G.Y. Effect of degassing on water droplets stability in crude oil emulsion with dissolved CO<sub>2</sub>. *J. Pet. (Pet. Process.)* **2022**, *38*, 834–845.
8. Shrivastava, K.; Hwang, J.; Mukul, S. Formation of Complex Fracture Networks in the Wolfcamp Shale: Calibrating Model Predictions with Core Measurements from the Hydraulic Fracturing Test Site. In Proceedings of the SPE Annual Technical Conference and Exhibition, Dallas, TX, USA, 24–26 September 2018.
9. Wu, Y.H.; Gong, F.; Xia, K.J.; Zhang, J.; Wang, C.Y.; Wen, S.C. Study on the adaptability of a nano-silica-based microemulsion for low permeability reservoirs with reduced pressure and increased injection. *Drill. Extr. Technol.* **2020**, *43*, 111–114+117.
10. Dai, C.L.; Wang, S.L.; Li, Y.Y.; Gao, M.W.; Liu, Y.F.; Sun, Y.P.; Zhao, M.W. The first study of surface modified silica nanoparticles in pressure-decreasing application. *RSC Adv.* **2015**, *5*, 61838–61845. [[CrossRef](#)]
11. Wang, T.R.; Zhang, Y.; Li, L.; Yang, Z.; Liu, Y.F.; Fang, J.C.; Dai, C.L.; You, Q. Experimental study on pressure-decreasing performance and mechanism of nanoparticles in low permeability reservoir. *J. Pet. Sci. Eng.* **2018**, *166*, 693–703. [[CrossRef](#)]
12. Yang, J.B.; Hou, J.R.; Qu, M.; Wen, Y.C.; Liang, T.; Wu, W.P.; Zhao, M.D.; Yang, E.L. Evaluation of 2-D smart nano black card for oil drive performance in low permeability reservoirs. *Oilfield Chem.* **2020**, *37*, 305–310.
13. Tangirala, S.; Sheng, J.J. Roles of surfactants during soaking and post leak-off production stages of hydraulic fracturing operation in tight oil-wet rocks. *Energy Fuels* **2019**, *33*, 8363–8373. [[CrossRef](#)]
14. Shuler, P.J.; Lu, Z.; Ma, Q.S.; Tang, Y.C. Surfactant Huff-n-Puff Application Potentials for Unconventional Reservoirs. In Proceedings of the SPE Improved Oil Recovery Conference, Tulsa, OK, USA, 11–13 April 2016.
15. Kim, J.; Zhang, H.; Sun, H.; Li, B.; Paul, C. Choosing Surfactants for the Eagle Ford Shale Formation: Guidelines for Maximizing Flowback and Initial Oil Recovery. In Proceedings of the SPE Low Perm Symposium, Denver, CO, USA, 5–6 May 2016.
16. Alvarez, J.O.; Saputra, I.W.; Schechter, D.S. The Impact of Surfactant Imbibition and Adsorption for Improving Oil Recovery in the Wolfcamp and Eagle Ford Reservoirs. *SPE J.* **2018**, *23*, 2103–2117. [[CrossRef](#)]
17. Wang, Z.; Cao, G.S.; Bai, Y.J.; Wang, P.L.; Wang, X. Current status and outlook of enhanced recovery technology in low permeability reservoirs. *Spec. Oil Gas Reserv.* **2023**, *30*, 1–13.
18. Ren, K.F.; Shu, F.C.; Lin, K.X.; Luo, G.; Xiang, X.J. Surface modified decompression and augmented injection technology suitable for water injection wells in thick oil reservoirs. *Sci. Technol. Eng.* **2016**, *16*, 70–74.
19. Shang, D.S.; Hou, J.R.; Cheng, T.T. Performance of SiO<sub>2</sub> nanofluid in low-permeability reservoirs for oil drive and optimization of injection parameters. *Oilfield Chem.* **2021**, *38*, 137–142.
20. Zhang, X.; Liu, D.X.; Li, L.L.; Liu, Y.; Yu, P.H.; Xu, J.J.; Zhou, H.; Yuan, J. Synergistic effects of surfactants on depressurization and augmented injection in high salinity low-permeability reservoirs: Formula development and mechanism study. *Colloids Surf. A Physicochem. Eng. Asp.* **2021**, *628*, 127312.
21. Yousef, K.; Sanaz, S.; Masoud, R.; Mohammad, S. Review on application of nanoparticles for EOR purposes: A critical review of the opportunities and challenges. *Chin. J. Chem. Eng.* **2019**, *27*, 237–246.
22. Yu, H.T.; He, Y.B.; Liu, Y.M.; Zhang, T.J. Experiment on high temperature and high-pressure dynamic throughput percolation oil drive in ultra-low permeability reservoir. *Daqing Pet. Geol. Dev.* **2022**, *41*, 80–86.
23. Ahmadi, S.; Hosseini, M.; Tangestan, E.; Ebrahim Mousavi, S.; Niazi, M. Wettability alteration and oil recovery by spontaneous imbibition of smart water and surfactants into carbonates. *Pet. Sci.* **2020**, *17*, 712–721. [[CrossRef](#)]
24. Liu, J.; Sheng, J.J.; Huang, W. Experimental investigation of microscopic mechanisms of surfactant-enhanced spontaneous imbibition in shale cores. *Energy Fuels* **2019**, *33*, 7188–7199. [[CrossRef](#)]
25. Wu, C.P.; Ye, Z.B.; Nie, X.T.; Liu, D.; Lai, N.J. Synthesis and evaluation of depressurization and injection treatment agent suitable for low-permeability reservoirs. *Chem. Phys. Lett.* **2022**, *804*, 139904. [[CrossRef](#)]
26. Carpenter, C. Designing an Optimized Surfactant Flood in the Bakken. *J. Pet. Technol.* **2016**, *68*, 58–92. [[CrossRef](#)]
27. Shang, D.S.; Yi, Z.; Liu, X.; Yang, J.B.; Hu, X.N.; Zhang, R.Q. Research progress of nanofluids for oil repelling in low permeability reservoirs. *Petrochemicals* **2023**, *52*, 131–137.
28. Li, Y.C.; Li, Q.; Zhang, W.D.; Bao, X.N.; Jin, J.; Meng, Y.; Sha, O. Development and application of in-situ microemulsion pressure-relief and injection relief agent for ultra-high temperature and ultra-low permeability reservoirs. In *Chinese Chemical Society: Proceedings of the Sixteenth Conference on Colloid and Interfacial Chemistry of the Chinese Chemical Society—Session VI: Applied Colloid and Interfacial Chemistry, Qingdao, China, 25–28 July 2017*; Chinese Chemical Society: Beijing, China, 2017; p. 2.

**Disclaimer/Publisher’s Note:** The statements, opinions and data contained in all publications are solely those of the individual author(s) and contributor(s) and not of MDPI and/or the editor(s). MDPI and/or the editor(s) disclaim responsibility for any injury to people or property resulting from any ideas, methods, instructions or products referred to in the content.